INSTITUTE OF PHYSICS PUBLISHING MEASUREMENT SCIENCE AND TECHNOLOGY
Meas. Sci. Technol. **13** (2002) 1124–1131 PII: S0957-0233(02)29812-4

Calibration of flux-gate magnetometers using relative motion

H U Auster[1], K H Fornacon[1], E Georgescu[2], K H Glassmeier[1] and U Motschmann[3]

[1] Institut für Geophysik und Meteorologie, TU Braunschweig, Mendelssohnstr. 3, Germany
[2] Max Planck Institut für Extraterrestrische Physik Garching, Giessenbachstrasse Postfach 1603, Germany
[3] Institut für Theoretische Physik, TU Braunschweig, Mendelssohnstr. 3, Germany

Received 16 October 2001, in final form 2 April 2002, accepted for publication 22 April 2002
Published 20 June 2002
Online at stacks.iop.org/MST/13/1124

Abstract
A simple analytical model for the calibration of a flux-gate magnetometer using relative sensor motion in a constant magnitude magnetic field (B) is presented.

Sensor motion is parametrized in terms of elementary rotations about one axis. The number of elementary rotations constitutes the number of degrees of freedom of the motion.

A generalization is performed by investigating cases with known/unknown B, one/several different values of B, one/several degrees of freedom. The maximum number of calibration parameters, which can be determined in each case, is established.

The conclusion is that the determination of all calibration parameters, i.e. an absolute calibration of the instrument, is already possible if the relative motion has at least two degrees of freedom at a known, constant B value.

Two experimental applications of the model are described briefly.

Keywords: calibration, fluxgate magnetometer

1. Introduction

Calibration means relating the output of a magnetometer ($\boldsymbol{B}_M$) to the value of the external field ($\boldsymbol{B}$) to be measured in a reference system. Mathematically this can be expressed with a linear equation as follows:

$$\begin{aligned} \boldsymbol{M}_P(\boldsymbol{B}_M - \boldsymbol{Z}_P) &= \boldsymbol{B} \\ \boldsymbol{O}_P\boldsymbol{S}_P(\boldsymbol{B}_M - \boldsymbol{Z}_P) &= \boldsymbol{A}\boldsymbol{B}. \end{aligned} \tag{1}$$

The matrix $\boldsymbol{M}_P$ with nine elements was decomposed into three matrices $\boldsymbol{O}$, $\boldsymbol{S}$ and $\boldsymbol{A}$. Each of these matrices contains three significant elements (besides unity and zero elements). $\boldsymbol{O}$ is a triangular matrix which has unity for all its principal diagonal elements, $\boldsymbol{S}$ is a diagonal matrix and $\boldsymbol{A}$ is a rotation matrix defining the transformation from the reference system of $\boldsymbol{B}$ to the orthogonal sensor system using three Euler angles. $\boldsymbol{Z}_P$ is the vector containing the three components of the sensor offset, i.e. the output for $\boldsymbol{B} = 0$. The index 'P' means that all quantities are real physical errors. The assumption of a linear transfer function is justified by the sensor internal field feedback.

The vector relation written above is a system of three linear equations. The left-hand sides of these equations contain the nine unknown calibration parameters; i.e. we need at least three independent values for the right-hand side in order to determine them. To get three (or more) independent values for the right-hand side we usually need an experimental setup allowing a precise measurement of all involved experimental quantities (e.g. currents and geometry in a coil system) and the possibility to change them in a highly controlled way. Since the right-hand side contains both the attitude and the field, it can be sufficient to modify only one of them. Calibration methods using either the modification of $\boldsymbol{A}$ or $\boldsymbol{B}$ are given in the following three examples.

(1) $\boldsymbol{A}$ = constant, modification of $\boldsymbol{B}$ using the natural variation of the Earth's field: $\boldsymbol{B}$ is determined by a reference instrument, such as, for example, in the variometer intercomparisons performed every two years

in the IAGA workshops on geomagnetic observatory instruments (Rasson 1996, Linthe 1998).

(2) $\boldsymbol{A}$ = constant, modification of $\boldsymbol{B}$ in a coil system: $\boldsymbol{B}$ is determined by measuring the current in the coils, such as, for example, in the calibration facility of TU Braunschweig (Kertz *et al* 1968).

(3) $\boldsymbol{B}$ = constant, modification of $\boldsymbol{A}$ by rotating the sensor: the offsets can be determined by rotating the sensor about 180° in reduced fields. Orthogonality and scaling coefficients are negligible in reduced fields.

This paper proposes and analyses a method based on the invariance of the field magnitude (B = constant) and the motion of the sensor. The sensor motion is parametrized in terms of elementary rotations. The rotation angle should be not a measured input quantity ($\boldsymbol{A}$ is variable and unknown). Therefore, only the magnitude of the field can be extracted from the right-hand side of equation (1). Instead of three vector equations, nine scalar equations are needed to determine all calibration parameters. The scalar calibration of vector magnetometers was already successfully applied to magnetometers mainly for near-Earth space missions (Georgescu 1995, Auster *et al* 1998, Merayo *et al* 2000). In this paper the relation between sensor motion and the possibility of determining the calibration parameters will be analysed. The model assumption of constant B (a 'worst case' assumption) imposes a constraint for $\boldsymbol{B}$, but any result remains valid if the real measurement is performed at different known field magnitudes. On the other hand, the assumption of variable but unknown $\boldsymbol{A}$ simplifies significantly the requirements for the measurement facility. It is an extension of similar algorithms (Davis and Smith 1968, Hedgecock 1975, Lerner and Shuster 1981, Shuster 1981, Thompson *et al* 1984, Davenport *et al* 1991) which were used for in-flight offset determination, such that now the full set of errors (offset, scale factor error and nonorthogonality) can be determined. The proposed method is applicable for all vector magnetometers, but not for variometers with static field compensation.

2. Description of the algorithm

In analogy to equation (1) we can express $\boldsymbol{B}_M$ as a function of numerically estimated errors (index 'N'):

$$\boldsymbol{O}_N\boldsymbol{S}_N(\boldsymbol{B}_M - \boldsymbol{Z}_N) = \boldsymbol{A}\boldsymbol{B}. \tag{2}$$

Combining equations (1) and (2), we get

$$\boldsymbol{O}_P\boldsymbol{S}_P\boldsymbol{S}_N^{-1}\boldsymbol{O}_N^{-1}\boldsymbol{A}\boldsymbol{B} + \boldsymbol{O}_P\boldsymbol{S}_P(\boldsymbol{Z}_N - \boldsymbol{Z}_P) = \boldsymbol{A}\boldsymbol{B}. \tag{3}$$

We rewrite the equation for simplicity, replacing the ratios and differences of physical and estimated quantities $\boldsymbol{O}_P\boldsymbol{S}_P\boldsymbol{S}_N^{-1}\boldsymbol{O}_N^{-1}$ by $\boldsymbol{O}\boldsymbol{S}$ and $\boldsymbol{O}_P\boldsymbol{S}_P(\boldsymbol{Z}_N - \boldsymbol{Z}_P)$ by $\boldsymbol{Z}$ and call them calibration errors. If the estimates compensate the physical calibration parameters the matrices $\boldsymbol{S}$ and $\boldsymbol{O}$ become identity matrices and the offset $\boldsymbol{Z}$ a zero vector. The square of equation (3) reads

$$[\boldsymbol{O}\boldsymbol{S}\boldsymbol{A}\boldsymbol{B} + \boldsymbol{Z}]^{\mathrm{T}}[\boldsymbol{O}\boldsymbol{S}\boldsymbol{A}\boldsymbol{B} + \boldsymbol{Z}] = |\boldsymbol{B}|^2. \tag{4}$$

The only time-dependent quantity is the attitude $\boldsymbol{A}$ since we work with the assumption of constant B and constant calibration coefficients. In order to take into account this time dependence explicitly we parametrize the attitude matrix $\boldsymbol{A}$ by introducing the Euler angles φ, ψ, ϑ, written as

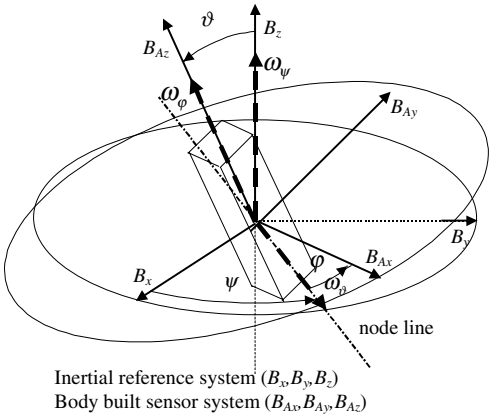

Figure 1. Attitude parametrization by means of Euler angles.

$$\varphi = \omega_\varphi t; \qquad \psi = \omega_\psi t; \qquad \vartheta = \omega_\vartheta t, \tag{5}$$

where $\omega_\varphi, \omega_\psi, \omega_\vartheta$ are independent angular velocities of the elementary rotations (see figure 1). Since the field magnitude during the calibration is constant, we can write

$$\frac{\partial|\boldsymbol{B}|^2}{\partial t} = 0. \tag{6}$$

Combining equations (5) and (6) we get the following equation for the derivative:

$$\frac{\partial|\boldsymbol{B}|^2}{\partial t} = \omega_1\frac{\partial|\boldsymbol{B}|^2}{\partial\varphi} + \omega_2\frac{\partial|\boldsymbol{B}|^2}{\partial\psi} + \omega_3\frac{\partial|\boldsymbol{B}|^2}{\partial\vartheta} = 0. \tag{7}$$

Based on the assumed independence of the angular velocities we get the following three equations:

$$\frac{\partial|\boldsymbol{B}|^2}{\partial\varphi} = 0, \qquad \frac{\partial|\boldsymbol{B}|^2}{\partial\psi} = 0 \qquad \text{and} \qquad \frac{\partial|\boldsymbol{B}|^2}{\partial\vartheta} = 0. \tag{8}$$

For each of the three equations we get four types of time dependencies (spectral frequencies): $\sin(\omega t)$, $\cos(\omega t)$, $\sin(2\omega t)$, $\cos(2\omega t)$. The only solution is to have the four coefficients of these trigonometric functions equal to zero. So we have as a whole a system consisting of a maximum 12 equations. If at least nine of them are independent we can determine all nine calibration coefficients.

In the following paragraph we analyse separately the influence of the different types of calibration parameters on the measured field magnitude. We define in each case the set of solutions and look for the intersection of the solution sets. We exemplify the processing with a rotation about B_z with angle ψ. The complete set of equations can be found in Auster (1999). For the graphical representation we always use the following parameters:

$\varphi = 30°$, $\quad B_x = -40$ nT
$\vartheta = -40°$, $\quad B_y = 20$ nT
$\quad B_z = 30$ nT.

2.1. Influence of the offsets

Neglecting in equation (4) the scaling and non-orthogonality errors we get

$$|\boldsymbol{B}|^2 = (B_{Ax} + Z_x)^2 + (B_{Ay} + Z_y)^2 + (B_{Az} + Z_z)^2. \qquad (9)$$

$\boldsymbol{B}_A$ stands for the product $\boldsymbol{AB}$, i.e. the magnetic field in the sensor system. The partial derivatives of $\boldsymbol{B}^2$ with respect to sine and cosine are linear in the components of $\boldsymbol{Z}$:

$$a_1^f Z_x + a_2^f Z_y + a_3^f Z_z = 0. \qquad (10)$$

The index 'f' of the coefficients a_i^f stands for the type of spectral term (the sine or cosine of the rotation or double rotation frequency) of the derivative. The coefficients of the sine and cosine terms are respectively expressed as

$$\begin{aligned} a_1^S &= -B_x \cos\varphi - B_y \sin\varphi \cos\vartheta \\ a_2^S &= B_x \sin\varphi - B_y \cos\varphi \cos\vartheta \\ a_3^S &= B_y \sin\vartheta \end{aligned} \qquad (11)$$

$$\begin{aligned} a_1^C &= -B_x \sin\varphi \cos\vartheta + B_y \cos\varphi \\ a_2^C &= -B_x \cos\varphi \cos\vartheta - B_y \sin\varphi \\ a_3^C &= B_x \sin\vartheta. \end{aligned} \qquad (12)$$

Both equations describe plane surfaces. Since the scalar product of the surface normals $(a_1^S a_1^C + a_2^S a_2^C + a_3^S a_3^C)$ is equal to zero, the surfaces are perpendicular.

Rewriting the equations with respect to B, we get

$$\begin{pmatrix} -Z_x \cos\varphi + Z_y \sin\varphi \\ (-Z_x \sin\varphi - Z_y \cos\varphi)\cos\vartheta + Z_z \sin\vartheta \end{pmatrix} \quad \begin{pmatrix} (-Z_x \sin\varphi - Z_y \cos\varphi)\cos\vartheta + Z_z \sin\vartheta \\ Z_x \cos\varphi - Z_y \sin\varphi \end{pmatrix} \begin{pmatrix} B_x \\ B_y \end{pmatrix} = 0. \qquad (13)$$

If we do not consider the trivial solutions $B_x = B_y = 0$, we get the conditions for the offsets by equating the matrix to zero. The determinant is equal to zero only if the offsets satisfy the following conditions:

$$-Z_x \cos\varphi + Z_y \sin\varphi = 0; \qquad Z_z\text{—arbitrary} \qquad (14)$$

$$(-Z_x \sin\varphi - Z_y \cos\varphi)\cos\vartheta + Z_z \sin\vartheta = 0. \qquad (15)$$

The solution set in the $\{Z_x, Z_y, Z_z\}$-space is the line of intersection of the two planes. This line coincides with the rotation axis (see figure 1). Since the solutions are along the rotation axis, one can determine the offsets only in the plane perpendicular to this axis. The component of the offset along the rotation axis (Z_z) is arbitrary. Similarly to the rotation around B_z with ψ, the rotation about the other two axes with φ, respectively ϑ define solution sets, which are also the intersection lines of two perpendicular planes, coinciding with the rotation axes. Thus, we can conclude the following.

Only the offsets perpendicular to the rotation axis can be determined in the case of motion with one degree of freedom; the offset component along the spin axis is arbitrary. The offset can be completely determined in the case of motion with two degrees of freedom. The point of intersection of the two lines, representing the solution sets, is the origin. This means that a rotation + nutation are enough to determine the offset. Three simultaneous rotations do not produce contradictions, since all intersection lines meet in the origin. A non-zero magnetic field is a necessary requirement. The field direction should not coincide with that of the spin axis in the case of one degree of freedom. If more than one degrees of freedom are present, alignment with one of the axes is allowed. The solutions for three rotations are depicted in figure 2. The line of intersection is each time the spin axis.

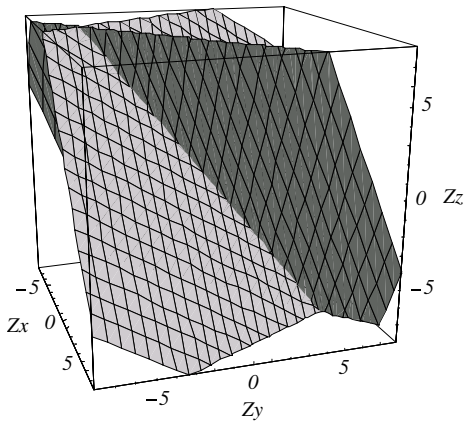

Figure 2. Graphical representation of the solutions of equation (10) with the parameter sets (11) and (12).

2.2. The influence of the scale factor

We repeat the procedure for the scale factors. Equation (4) becomes

$$|\boldsymbol{B}|^2 = (S_x B_{Ax})^2 + (S_y B_{Ay})^2 + (S_z B_{Az})^2. \qquad (16)$$

The partial derivative with respect to ψ gives four quadratic equations, of the form

$$a_{11}^f S_x^2 + a_{22}^f S_y^2 + a_{33}^f S_z^2 = 0. \qquad (17)$$

The coefficients a_{ii}^f are calculated as follows:

$$\begin{aligned} a_{11}^S &= (-B_y \sin 2\vartheta (1 - \cos 2\varphi) - 2B_x \sin\vartheta \sin 2\varphi) B_z \\ a_{22}^S &= (-B_y \sin 2\vartheta (1 + \cos 2\varphi) + 2B_x \sin\vartheta \sin 2\varphi) B_z \\ a_{33}^S &= (2B_y \sin 2\vartheta) B_z \end{aligned} \qquad (18)$$

$$\begin{aligned} a_{11}^C &= (-B_x \sin 2\vartheta (1 - \cos 2\varphi) + 2B_y \sin\vartheta \sin 2\varphi) B_z \\ a_{22}^C &= (-B_x \sin 2\vartheta (1 + \cos 2\varphi) - 2B_y \sin\vartheta \sin 2\varphi) B_z \\ a_{33}^C &= (2B_x \sin 2\vartheta) B_z \end{aligned} \qquad (19)$$

$$\begin{aligned} a_{11}^{2S} &= -(B_x^2 - B_y^2)((1 - \cos 2\vartheta) + \cos 2\varphi (3 + \cos 2\vartheta)) \\ &\quad - 8B_x B_y \cos\vartheta \sin 2\varphi \\ a_{22}^{2S} &= -(B_x^2 - B_y^2)((1 - \cos 2\vartheta) - \cos 2\varphi (3 + \cos 2\vartheta)) \\ &\quad + 8B_x B_y \cos\vartheta \sin 2\varphi \\ a_{33}^{2S} &= 2(B_x^2 - B_y^2)(1 - \cos 2\vartheta) \end{aligned} \qquad (20)$$

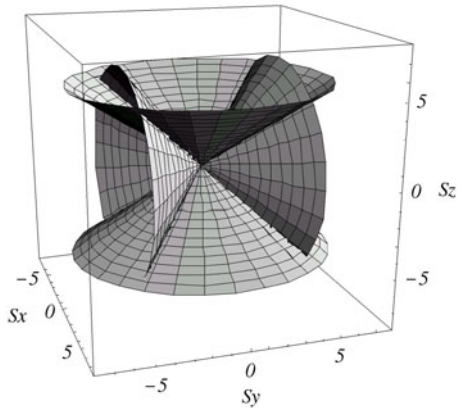

Figure 3. Graphical representation of the solutions of equation (17) with the parameter sets (18) and (19).

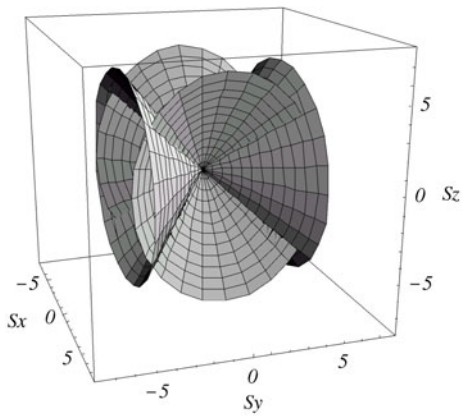

Figure 4. Graphical representation of the solutions of equation (17) with the parameter sets (20) and (21).

$$
\begin{aligned}
a_{11}^{2C} &= 2B_xB_y((1-\cos 2\vartheta)+\cos 2\varphi(3+\cos 2\vartheta)) \\
&\quad -\ 4(B_x^2-B_y^2)\cos\vartheta\sin 2\varphi \\
a_{22}^{2C} &= 2B_xB_y((1-\cos 2\vartheta)-\cos 2\varphi(3+\cos 2\vartheta)) \\
&\quad +\ 4(B_x^2-B_y^2)\cos\vartheta\sin 2\varphi \\
a_{33}^{2C} &= -4B_xB_y(1-\cos 2\vartheta).
\end{aligned}
\tag{21}
$$

In each case the solutions are surfaces of second order, with non-zero main axis coefficients, which can be represented geometrically as elliptical double cones.

Substituting in the parameter set (19) B_x with B_y and B_y with $-B_x$, one gets the parameter set (18). Consequently the solutions of equation (17) with parameters (18) and (19) are two identical double cones perpendicular to each other. The symmetry point coincides with the origin and the common solutions are the diagonals of the $\{S_x, S_y, S_z\}$-space. In the case of the double rotation frequency the result is the same.

Substituting in (21) the expression $2B_xB_y$ by $-(B_x^2-B_y^2)$ and $(B_x^2-B_y^2)$ by $2B_xB_y$, one gets (20). Hence the two perpendicular double cones intersect again on the diagonals of the $\{S_x, S_y, S_z\}$-space. The two cases (simple and double rotation frequency) produce the same results, i.e. the two systems of equations are not independent. The solution sets are shown in figures 3 and 4. An absolute determination of the scale factors is not possible, just a relative one. The trivial solution $B_x = B_y = 0$ has to be excluded. For $B_z = 0$ the solution sets of the simple rotation frequency are missing.

We can conclude that a relative determination of the scale factors is possible in the case of motion with one degree of freedom. Additional degrees of freedom do not reduce the solution sets, which coincide with the space diagonals. The magnetic field must be non-zero and its direction non-aligned to the rotation axis.

2.3. Influence of the non-orthogonality

If only the non-orthogonality $(O_x,\ O_y,\ O_z)$ is kept in the equation of the field magnitude, the expression becomes

$$
|\boldsymbol{B}|^2 = (B_{Ax})^2+(O_{xy}B_{Ax}+B_{Ay})^2+(O_{xz}B_{Ax}+O_{yz}B_{Ay}+B_{Az})^2. \tag{22}
$$

The ψ derivation of the field magnitude is given by four equations of the type

$$
\begin{aligned}
&a_{11}^f O_{xy}^2 + a_{22}^f O_{xz}^2 + a_{33}^f O_{yz}^2 + 2a_1^f(O_{xz}O_{yz}+O_{xy}) \\
&\quad + 2a_2^f O_{xz} + 2a_3^f O_{yz} = 0.
\end{aligned}
\tag{23}
$$

We perform a principal axes transformation, because this simplifies the interpretation of the surfaces. In this temporary coordinate system the surfaces have the following equation:

$$
d_{11}^f\tilde{x}^2 + d_{22}^f\tilde{y}^2 + d_{33}^f\tilde{z}^2 + b_0 = 0. \tag{24}
$$

The parameters are transformed as follows:

$$
\begin{aligned}
d_{11}^f &= a_{11}^f \\
d_{22}^f &= \tfrac{1}{2}\Big(a_{22}^f + a_{33}^f - \sqrt{(a_{22}^f)^2 - 2a_{22}^f a_{33}^f + (a_{33}^f)^2 + 4(a_1^f)^2}\Big) \\
d_{33}^f &= \tfrac{1}{2}\Big(a_{22}^f + a_{33}^f \\
&\quad + \sqrt{(a_{22}^f)^2 - 2a_{22}^f a_{33}^f + (a_{33}^f)^2 + 4(a_1^f)^2}\Big) \\
b_0 &= -\frac{(a_1^f)^2}{a_{11}^f} + \frac{a_{33}^f(a_2^f)^2 + a_{22}^f(a_3^f)^2 - 2a_1^f a_2^f a_3^f}{(a_1^f)^2 - a_{22}^f a_{33}^f}.
\end{aligned}
\tag{25}
$$

If the derived surfaces are different then the corresponding equations are independent.

We get the following parameters of the second-order surfaces:

$$
\begin{aligned}
d_{11}^S &= -8\sin\varphi\sin\vartheta(B_x\cos\varphi + B_y\sin\varphi\cos\vartheta) \\
d_{22}^S &= -2B_y\sin 2\vartheta - \sqrt{16B_x^2\sin^2\vartheta + 4B_y^2\sin^2 2\vartheta} \\
d_{22}^S &= -2B_y\sin 2\vartheta + \sqrt{16B_x^2\sin^2\vartheta + 4B_y^2\sin^2 2\vartheta} \\
b_0^S &= -4B_y\sin 2\vartheta + \frac{\sin\vartheta(B_x\cos 2\varphi + B_y\sin 2\varphi\cos\vartheta)^2}{\sin\varphi(B_x\cos\varphi + B_y\sin\varphi\cos\vartheta)}
\end{aligned}
\tag{26}
$$

$$
\begin{aligned}
d_{11}^C &= -8\sin\varphi\sin\vartheta(B_y\cos\varphi - B_x\sin\varphi\cos\vartheta) \\
d_{22}^C &= 2B_x\sin 2\vartheta - \sqrt{16B_y^2\sin^2\vartheta + 4B_x^2\sin^2 2\vartheta} \\
d_{33}^C &= 2B_x\sin 2\vartheta + \sqrt{16B_y^2\sin^2\vartheta + 4B_x^2\sin^2 2\vartheta} \\
b_0^C &= 4B_x\sin 2\vartheta + \frac{\sin\vartheta(B_y\cos 2\varphi - B_x\sin 2\varphi\cos\vartheta)^2}{\sin\varphi(B_y\cos\varphi - B_x\sin\varphi\cos\vartheta)}
\end{aligned}
\tag{27}
$$

$$
\begin{aligned}
d_{11}^{2S} &= -8((B_x + B_y)\cos\varphi - (B_x - B_y)\cos\vartheta\sin\varphi) \\
&\quad \times ((B_x - B_y)\cos\varphi + (B_x + B_y)\cos\vartheta\sin\varphi) \\
d_{22}^{2S} &= -4(B_x^2 - B_y^2)\sin^2\vartheta \\
&\quad - 4\sqrt{4(B_x^2 + B_y^2)^2\cos^2\vartheta + (B_x^2 - B_y^2)^2\sin^4\vartheta} \\
d_{33}^{2S} &= -4(B_x^2 - B_y^2)\sin^2\vartheta \\
&\quad + 4\sqrt{4(B_x^2 + B_y^2)^2\cos^2\vartheta + (B_x^2 - B_y^2)^2\sin^4\vartheta} \\
b_0^{2S} &= -8(B_x^2 - B_y^2)\sin^2\vartheta + \{[((B_x^2 - B_y^2) \\
&\quad \times (3 + \cos 2\vartheta)\sin 2\varphi - 8B_xB_y\cos\vartheta\cos 2\varphi)^2] \\
&\quad \times [2((B_x + B_y)\cos\varphi - (B_x - B_y)\cos\vartheta\sin\varphi) \\
&\quad \times ((B_x - B_y)\cos\varphi + (B_x + B_y)\cos\vartheta\sin\varphi)]^{-1}\}
\end{aligned}
\tag{28}
$$

$$
\begin{aligned}
d_{11}^{2C} &= 8(B_x\cos\varphi + B_y\cos\vartheta\sin\varphi) \\
&\quad \times (B_y\cos\varphi - B_x\cos\vartheta\sin\varphi) \\
d_{22}^{2C} &= 4B_xB_y\sin^2\vartheta \\
&\quad - 4\sqrt{(B_x^2 + B_y^2)^2\cos^2\vartheta + (B_xB_y)^2\sin^4\vartheta} \\
d_{33}^{2C} &= 4B_xB_y\sin^2\vartheta \\
&\quad + 4\sqrt{(B_x^2 + B_y^2)^2\cos^2\vartheta + (B_xB_y)^2\sin^4\vartheta} \\
b_0^{2C} &= 8B_xB_y\sin^2\vartheta - \{[(2(B_x^2 - B_y^2)\cos 2\varphi\cos\vartheta \\
&\quad + B_xB_y(3 + \cos 2\vartheta)\sin 2\varphi)^2][2(B_x\cos\varphi \\
&\quad + B_y\cos\vartheta\sin\varphi)(B_y\cos\varphi - B_x\cos\vartheta\sin\varphi)]^{-1}\}.
\end{aligned}
\tag{29}
$$

The dominant terms in the parameters d_{22}^f and d_{33}^f are the square roots, which means that d_{22}^f is always negative and d_{33}^f is always positive. Since the signs of d_{11}^f and b_0^f are arbitrary, the solution set can be represented as a one- or a two-shell hyperboloid. The common solution is the intersection of these four surfaces. The origin in the O_{xy}, O_{xz}, O_{yz}-space constitutes in each case the common solution. Another common solution cannot be excluded based on theoretical considerations. The solution sets are represented in figures 5 and 6. Non-orthogonality produces both the single and the double rotation frequency in the magnitude. Hence four equations are available for the determination of this error. The solutions are four independent surfaces in the $\{O_{xy}, O_{xz}, O_{yz}\}$-space. Three surfaces are already enough for an absolute determination of the non-orthogonality parameters.

We can conclude that a simple rotation is enough for an absolute determination of the non-orthogonality. The system is over-determined, but there is one common solution which satisfies all equations and that is the origin. The magnetic field has to be non-zero and must have a direction not coincident with that of the spin axis. Introducing additional degrees of freedom, the degree of over-determination increases and the condition of no spin axis oriented magnetic field vanishes.

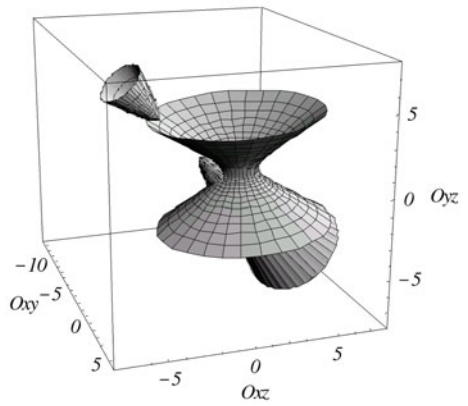

Figure 5. Graphical representation of the solutions of equation (24) with the parameter sets (26) and (27) re-transformed in the $\{O_{xy}, O_{xz}, O_{yz}\}$-space.

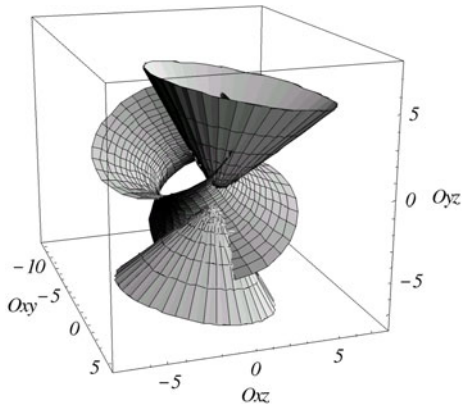

Figure 6. Graphical representation of the solutions of equation (24) with the parameter sets (28) and (29) re-transformed in the $\{O_{xy}, O_{xz}, O_{yz}\}$-space.

3. Experimental applications

We present two experimental applications. One concerns a ground-based magnetometer, designed for the research vessel Polarstern, and the other a space magnetometer, situated on-board the Equator-S satellite. The Polarstern magnetometer (70 000 nT range, 0.1 nT resolution) is equipped with digital fluxgate electronics. The Equator-S magnetometer is a classical analogue instrument with two ranges (2000 and 30 000 nT) and a 16 bit AD converter.

In the first example, the sensor was placed on a pillar and turned manually in about 30 different positions in an arbitrary way. In each of these positions one measurement was performed. Since the sensor was in a static position during the measurement, the dynamic behaviour of the instrument can be neglected. The field magnitude was monitored by a proton magnetometer. The calibration of the Polarstern magnetometer is based on a maximum number of inputs (i.e. motion with three degrees of freedom + known field magnitude). The second example, the in-flight calibration of a magnetometer on a spinning spacecraft, is based on a minimum number of inputs (i.e. motion with one degree of freedom + unknown field magnitude). In both cases the

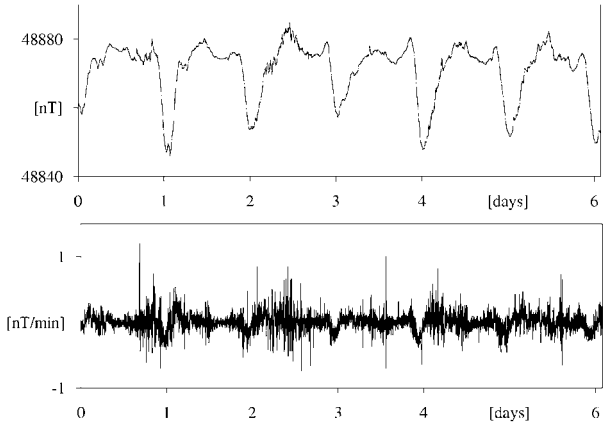

Figure 7. Magnetic field magnitude variation per minute ($\Delta B/\Delta t$) for six consecutive days. The measurements were made at Niemegk with an optically pumped tandem magnetometer (Pulz *et al* 1999). The average of the absolute variation is 0.1 nT min^{-1} with a standard deviation of 0.1 nT min^{-1}.

magnetic field has been assumed as 'constant' during the measurement. The measurement interval for the ground-magnetometer calibration was of the order of 2 min. To justify the assumptions of constant field a plot of the magnetic field magnitude variation per minute ($\Delta B/\Delta t$) is shown for six consecutive days in figure 7. The average of the absolute variation is 0.1 nT min^{-1} with a standard deviation of 0.1 nT min^{-1}. It means that an accuracy of 1 nT can be achieved with just one measurement with the proton magnetometer at the beginning or the end of he measurement cycle.

The calibration of the space-borne magnetometer was performed in weak magnetic fields at apogee of the orbit at a distance of 12 Earth radii. The measurement interval was on the order of seconds, short enough to have constant field, but long enough to have significant position changes, since the spinning period was 1.4 s.

Using the estimates introduced in equation (2) the following expression has to be minimized for all vectors of the time series of $\boldsymbol{B}_{Mi}$:

$$[\boldsymbol{O}_N\boldsymbol{S}_N(\boldsymbol{B}_{Mi}-\boldsymbol{Z}_N)]^{\mathrm{T}}[\boldsymbol{O}_N\boldsymbol{S}_N(\boldsymbol{B}_{Mi}-\boldsymbol{Z}_N)]-B^2=\Delta B_i^2. \tag{30}$$

The measured magnitude would be constant if no calibration errors were present. If the estimates are good, the variance of the magnitude is equal to zero:

$$\sigma^2=\sum_i(\Delta B_i^2)^2. \tag{31}$$

In a minimum variance analysis, the numerical estimates $\boldsymbol{Z}_N$, $\boldsymbol{S}_N$ and $\boldsymbol{O}_N$ are varied until the minimum of the variance is reached. In the case of unknown B the magnitude is treated as an additional free parameter, besides the calibration parameters. The sensitivity of the variance to the different calibration parameters is represented by the deviation of the estimated parameters from the physical ones.

In the case of the Polarstern magnetometer, the fit converges quickly and the reproducibility of the results is very good. With the best estimates the standard deviation (σ) of the magnitude is 1 nT. This contains the other, non-considered, errors (nonlinearity, inhomogeneity of the field).

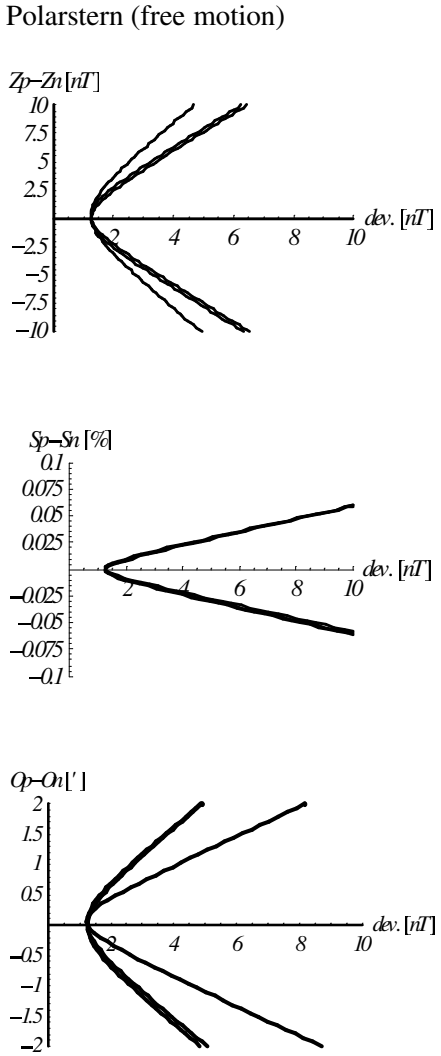

Figure 8. Standard deviation of the magnitude versus calibration errors of the Polarstern magnetometer (three components for each type).

The sensitivity of the method with respect to the different errors is shown in figure 8. The square root of the variance, i.e. the standard deviation, is represented on the x-axis, and the calibration error on the y-axis. The precision of the estimation is inversely proportional to the angle between the two branches of the curve. The precision is better than 2 nT for the offset, 0.005% for the scale factor and 0.005° for the nonorthogonality.

The second example is a simple rotation (motion with one degree of freedom) in an unknown homogeneous field. The standard deviation is again represented versus the different calibration errors (see figure 9). The offset component along the spin axis, as well as the scale factor, does not affect the time dependence of the magnitude. The non-orthogonality can be determined. The magnetometer noise level determines the overall error. The standard deviation is 60 pT. The offsets perpendicular to the spin axis can be determined with an accuracy of 0.02 nT. The accuracy of the determination of scale factor and non-orthogonality depends on the ratio of noise level and field magnitude; in this case it is 10^{-3}.

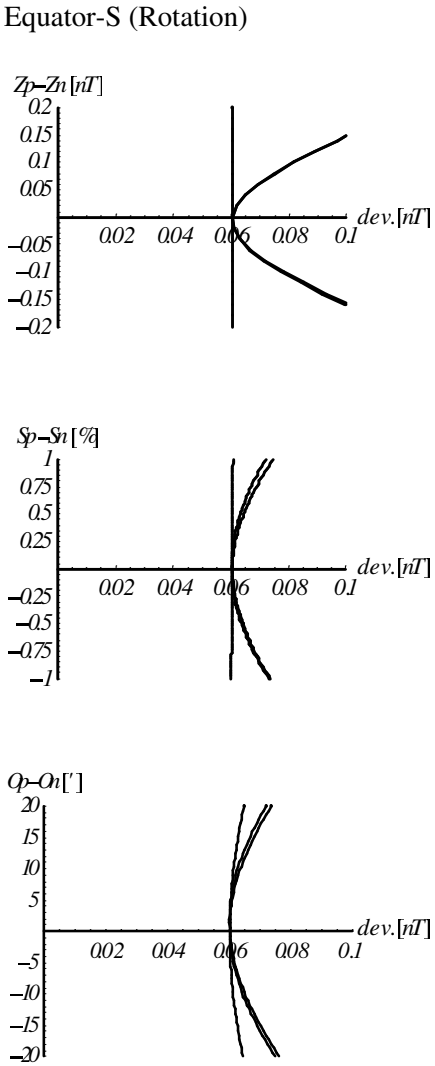

Figure 9. Standard deviation of the magnitude versus calibration errors of the Equator-S magnetometer (three components for each type).

4. Discussion

In the case of motion with one degree of freedom (magnetometer on a spinning spacecraft) we make use of four equations. Since we have altogether nine parameters, the complete determination of all the parameters is impossible. While the solution sets for the offsets and scale factors are not dependent on the magnetic field, those for the non-orthogonality are. Hence we can use additional equations to determine the non-orthogonality, if we perform measurements in various external fields. The four equations remain for the determination of the offset and scale factor and are enough to get the components perpendicular to the spin axis. If the magnitude of the magnetic field is known from an independent instrument (Overhauser magnetometer or Electron Drift Instrument) a fifth equation can be used. Measurements in various external fields allow the determination of the complete set of calibration parameters.

In the case of motion with two degrees of freedom (e.g. rotations with φ and ψ, ϑ = const.) we make use of eight equations for nine variables. For an absolute determination of the offsets and nonorthogonality a motion with two degrees of freedom is sufficient. Scale values can be determined only relatively. If the magnitude of the magnetic field is known we have nine equations for nine variables. Since the equations are independent, the solution is unique.

In the case of motion with three degrees of freedom (e.g. arbitrary rotation), we make use of 12 equations for nine variables. Solutions for offsets and non-orthogonality are over-determined, the solution for the scale values are still the diagonals of the $\{S_x, S_y, S_z\}$ space. In order to determine absolutely the scale factors the magnitude of the field has to be known. The situation is equivalent to the motion with two degrees of freedom.

We summarize the results for different cases in two tables. In table 1 we summarize the effects of different calibration errors on the time behaviour of the magnitude of the measured magnetic field, and the geometrical representation of the solution sets, as discussed in detail in section 2.

Possible solutions for different experimental situations are listed in table 2. Three cases which have high applicability are summarized:

(1) the rotation about two or three axes corresponds to an arbitrary sensor motion and may be used on the ground. In contrast to the traditional methods, it does not require sophisticated facilities,
(2) the rotation about one axis and
(3) the rotation about an axis which is aligned with a magnetometer axis, relating to the situation on a spinning spacecraft.

Table 1. Summary of motion dependences of B on calibration errors and geometrical representations of solution sets for $\mathrm{d}B/\mathrm{d}t = 0$.

Group of errors	Offset	Scaling factor	Nonorthogonality
Time dependences generated in the magnitude by the different errors	$\sin \omega t$ $\cos \omega t$	$\sin \omega t$ $\cos \omega t$ $\sin 2\omega t$ $\cos 2\omega t$	$\sin \omega t$ $\cos \omega t$ $\sin 2\omega t$ $\cos 2\omega t$
Surfaces in the solution space	Planes	Cones	Hyperboloids
Intersection of two surfaces	Line in the $\{Z_x, Z_y, Z_z\}$ space	Diagonals in the $\{S_x, S_y, S_z\}$ space	Curves in the $\{O_{xy}, O_{xz}, O_{yz}\}$ space
Intersection of three surfaces	Origin of the $\{Z_x, Z_y, Z_z\}$ space	Diagonals in the $\{S_x, S_y, S_z\}$ space	Origin of the $\{O_{xy}, O_{xz}, O_{yz}\}$ space

Table 2. Calibration possibilities for several experimental situations, the number of equations depending on the motion and B.

Type of motion	B known (+1 equation)		B unknown	
Rotation about three axes	12 + 1 equations		12 equations	
Rotation about two axes	8 + 1 equations		8 equations	
	Absolute	Relative	Absolute	Relative
	Z_x, Z_y, Z_z, S_x, S_y, S_z, O_{xy}, O_{xz}, O_{yz}	—	Z_x, Z_y, Z_z, O_{xy}, O_{xz}, O_{yz}	S_x, /S_y, / S_z
Rotation about one axis	$n(4+1)$ equations		$n4$ equations	
Rotation axis arbitrary	Absolute	Relative	Absolute	Relative
Several measurements (n) at different $\boldsymbol{B}$	Z_x, Z_y, Z_z, S_x, S_y, S_z, O_{xy}, O_{xz}, O_{yz}	—	Z_x, O_{xy}, O_{xz}, O_{yz}	Z_y/Z_z, $S_x/S_y/S_z$
Rotation about one axis	$n(4+1)$ equations		$n4$ equations	
Rotation axis $\parallel B_{R_z}$ axis	Absolute	Relative	Absolute	Relative
Several measurements (n) at different $\boldsymbol{B}$	Z_x, Z_y, Z_z, S_x, S_y, S_z, O_{xy}, O_{xz}, O_{yz}	—	Z_x, Z_y, O_{xy}, O_{xz}, O_{yz}	S_x/S_y

For the rotation about one axis, measurements at n different field values are investigated. Last but not least, the knowledge of the field magnitude was included. On the ground the magnitude information is mostly available by measurements with scalar magnetometers. The situation is different in space, where only a few satellites are equipped with scalar magnetometers. However, experiments such as the Electron Drift Instrument onboard Equator-S and Cluster also provide this information onboard spinning satellites.

For each of these cases the number of equations is given. Table 2 shows whether the parameter can be determined absolutely or if only ratios between parameters can be determined (relative parameter determination).

5. Conclusion

Sensor motion with two degrees of freedom (rotation about two axes) in a known constant field was found to be sufficient to determine all calibration parameters and thus absolutely calibrate a vector magnetometer. Using this fact, no coil systems to modify the field and no precise mechanics to turn the sensor about defined angles are necessary to calibrate the magnetometer. Consequently vector magnetometers with Earth field range can be calibrated everywhere if a proton magnetometer is available. This result of the model calculations has been verified in practice and a calibration accuracy of 1 nT was achieved. To increase the precision, the variation of the Earth field magnitude can be taken into account by repeated proton magnetometer measurements.

Furthermore, we presented a detailed description of the relationship between incorrect calibration parameters and the signatures of the sensor motion in the field magnitude. This is a welcomed input for the in-flight calibration of magnetometers on spinning spacecrafts.

References

Auster H U 1999 Kalibrierung von fluxgate magnetometern mittels relativbewegung zwischen sensor und magnetfeld *Dissertation an der TU Braunschweig* http://www.biblio.tu-bs.de/ediss/data/20000802a/20000802a.html

Auster H U, Georgescu E, Fornacon K H, Popescu D, Zarutski A, Hillenmaier O and Rustenbach J 1998 Calibration of fluxgate magnetometer using statistical methods (*Recordings During the 7th IAGA Workshop on Geomagnetic Observatory Instruments*) *GFZ Scientific Technical Report* (STR98/21)

Davenport P B, Rumpl W M and Welter G L 1991 In-flight determination of spacecraft magnetic bias independent of attitude *NASA* TN 5-26685 pp 326–43

Davis L and Smith E J 1968 The inflight determination of spacecraft field zeros *EOS Trans. Am. Geophys. Union* **49** 257

Georgescu E 1995 In-flight calibration technique for triaxial magnetometers applied to interball and Magiballs experiments *MPE Report* A10–95, pp 1–27

Hedgecock P C 1975 A correlation technique for magnetometer zero level determination *Space Sci. Instrum.* **1** 83

Kertz W, Lauche H and Maier A 1968 Magnetsrode, lage und einrichtung des magnetischen laboratoriums des instituts *GAMMA* 1(IGM der TU Braunschweig)

Lerner G M and Shuster M D 1981 Magnetometer bias determination and attitude determinationfor near-Earth spacecraft *J. Guid. Control* **4** 518–22

Linthe H J 1998 Results of the comparison measurements and the variometer test, recordings during the 7th IAGA workshop on geomagnetic observatory instruments *GFZ Scientific Technical Report* (STR98/21)

Merayo J M G, Brauer P, Primdahl F, Petersen J R and Nielsen O V 2000 Scalar calibration of vector magnetometers *Meas. Sci. Technol.* **11** 120–32

Pulz E, Jaeckel K-H and Linthe H-J 1999 A new optically pumped tandem magnetometer: principles and experiences *Meas. Sci. Technol.* **10** 1025–31

Rasson J L 1996 *Tests and Intercomparisons of Geomagnetic Instrumentation at the VIth Workshop of Magnetic Observatory Instruments, Data Acquisition and Processing*

Shuster M D 1981 Efficient algorithms for spin-axis attitude estimation *Flight Mechanics/Estimation Theory Symp. (NASA Goddard Space Flight Center, Greenbelt)*

Thompson R H, Neal G F and Shuster M D 1984 Magnetometer bias determination and spin-axis attitude estimation for the AMPTE mission *J. Guidance* **7** (4) Eng. Notes 504–7